



## Interaction between the ionic liquids 1-alkyl-3-methylimidazolium tetrafluoroborate and Pluronic<sup>®</sup> P103 in aqueous solution: A DLS, SANS and NMR study

A. Parmar<sup>a,\*</sup>, V.K. Aswal<sup>b</sup>, P. Bahadur<sup>a</sup>

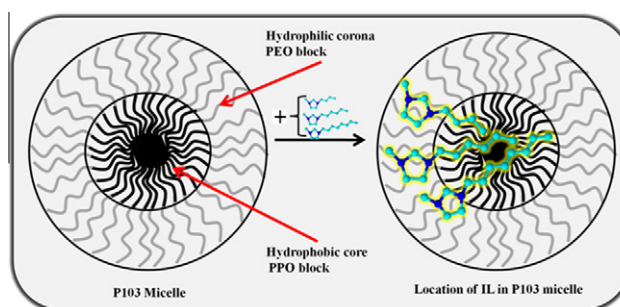
<sup>a</sup> Department of Chemistry, Veer Narmad South Gujarat University, Surat 395 007, India

<sup>b</sup> Solid State Physics Division, Bhabha Atomic Research Center, Mumbai 400 085, India

### HIGHLIGHTS

- ▶ Interaction of ILs with Pluronic micelles is proposed.
- ▶ Interaction studied by DLS, SANS, NMR technique.
- ▶ NOESY indicates PPO block interaction with alkyl group of IL.
- ▶ Through this kind of interactions, C<sub>n</sub>mim BF<sub>4</sub> and P103 can form mixed micelles.

### GRAPHICAL ABSTRACT



### ARTICLE INFO

#### Article history:

Received 22 March 2012  
 Received in revised form 16 May 2012  
 Accepted 29 May 2012  
 Available online 6 June 2012

#### Keywords:

P103 micelles  
 Ionic liquids  
 DLS  
 SANS  
 NOESY  
 Location

### ABSTRACT

The effect of three ionic liquids (ILs) 1-alkyl 3-methyl imidazolium tetrafluoroborates (C<sub>n</sub>mim BF<sub>4</sub>, n = 4, 6, 8) on micellar solutions of an ethylene oxide-propylene oxide block copolymer (PEO–PPO–PEO), Pluronic<sup>®</sup> P103 was examined from scattering and NMR techniques. The ILs alter the cloud point and micelle size dependant on their alkyl chain length and the results are discussed in terms of their behavior as cosolvent/cosurfactant. Cloud point data support the hydrogen bonding between the imidazolium cation and P103 while dynamic light scattering (DLS) and small angle neutron scattering (SANS) reveal that presence of ionic liquid is not conducive to the micelle formation of P103. The selective nuclear Overhauser effect (NOESY) indicates that the PPO block of the P103 interacts with the alkyl group of the C<sub>n</sub>mim<sup>+</sup> cation by hydrophobic interaction. Through this kind of interactions, C<sub>n</sub>mim BF<sub>4</sub> and P103 can form mixed micelles. This result indicates that the presence of ILs hinders the micelle formation of P103 in solution and promotes P103 to orient at air/water interface.

© 2012 Elsevier B.V. All rights reserved.

### Introduction

Ionic liquids (ILs) show high extractive selectivity, negligible volatility, inflammability, thermal stability etc., and thus play a promising role as alternative media in diverse areas [1]. One main aspect in IL research is the enormous cation-anion combinations, which result in a large potential for adjustability of structure/prop-

erties. ILs are often called 'designer solvents' or considered 'task-specific' because of their possibility to be tailored to fulfill the technological demands [2]. The most common ILs examined are made of 1-alkyl-3-imidazolium cations and halide (X<sup>-</sup>), tetrafluoroborate (BF<sub>4</sub><sup>-</sup>), phosphorus hexafluoride (PF<sub>6</sub><sup>-</sup>) or alkyl sulfate (RSO<sub>3</sub><sup>-</sup>) anions [3–5]. Surface active ionic liquids (SAILs) possess long alkyl chain in cation or anion [6,7] and form micelles in aqueous media [1–8], nonaqueous solvents [9] and other ionic liquids [10]. The investigation on the effect of ILs on the aggregation behavior of a surfactant could be helpful in enhancing the surfactant's properties and in widening its application in related industrial area.

\* Corresponding author. Tel.: +91 942 7777578; fax: +91 261 2256012.

E-mail addresses: [Arpan\\_parmar1985@yahoo.co.in](mailto:Arpan_parmar1985@yahoo.co.in) (A. Parmar), [vkaswal@yahoo.com](mailto:vkaswal@yahoo.com) (V.K. Aswal), [pbahadur2002@yahoo.com](mailto:pbahadur2002@yahoo.com) (P. Bahadur).

Pluronic® are ethylene oxide (EO) propylene oxide (PO) based FDA approved triblock copolymers (PEO–PPO–PEO) extensively studied in past two-three decades for their strongly temperature dependent micellization and thermoreversible rheological behavior in aqueous solutions [11]. The copolymers have gained much interest in recent years for their potential applications as vehicles in drug delivery systems [12], in the preparation of mesoporous and nanostructured materials [13].

Ionic liquids might modify micellar behaviour of PEO–PPO–PEO block copolymers, enrich the phase diagram and thus improve the performance of these block copolymers. However, there are few reports on micellar behavior of Pluronic® and other polyethylene oxide condensates in water-IL mixed solvents [14–19], and in pure ILs [20]. Zheng et al [19] have studied the effect of C<sub>4</sub>mim Br on the aggregation behavior of Pluronic® P104 aqueous solution and showed hydrophobic interaction of the PO block with butyl chain of C<sub>4</sub>mim cation (below 1.232 mol/L) leads to increase in micelle size and modulates the colloid chemical behavior of pluronic by altering hydrogen bond and hydrophobic interactions.

In this paper, we examined the influence of ionic liquids 1-butyl-3-methylimidazolium tetrafluoroborate (C<sub>4</sub>mim BF<sub>4</sub>), 1-hexyl-3-methylimidazolium tetrafluoroborate (C<sub>6</sub>mim BF<sub>4</sub>), 1-octyl-3-methylimidazolium tetrafluoroborate (C<sub>8</sub>mim BF<sub>4</sub>), on the clouding behavior and micellar characteristics of Pluronic® P103 in water. Dynamic light scattering (DLS) and small angle neutron scattering (SANS) were used to get information on micellar size and microstructure while 2D NMR (NOESY) was used to examine the interaction between ILs and P103. The aim of this study was to find the interaction mechanism between ionic liquid and PEO–PPO–PEO block copolymer, in order to use ionic liquid to control the properties of the polymeric micelle.

## Experimental

### Materials

Pluronic® P103 was received as a gift sample from BASF corp. Parsippany, NJ. The chemicals with preparation of IL (1-alkyl-3-methylimidazolium tetrafluoroborate) were of analytical grade and used without further purification.

### Methods

#### Cloud point

Cloud points (CPs) were determined by gently heating solution in thin 20 mL glass tube immersed in a beaker containing water well stirred with a magnetic bar while being heated. Temperature of the first appearance of turbidity was taken as the cloud point. The obtained results were reproducible up to ±0.5 °C.

#### Dynamic light-scattering (DLS) measurements

The DLS experiments were carried out at a fixed scattering angle of 90° on solutions using Zeta sizer Nano-ZS 4800 (Malvern Instruments, UK) equipped He–Ne laser operating at a wavelength of 633 nm. The average diffusion coefficients and hence the hydrodynamic size was obtained by the method of cumulants. Each measurement was repeated at least three-four times.

#### Small angle neutron scattering (SANS)

The mean incident wavelength ( $\lambda$ ) was 5.2 Å with wavelength resolution ( $\Delta \lambda/\lambda$ ) about 15% and scattering was measured in the Q range 0.017–0.35 Å<sup>-1</sup> (SANS facility at the DHRUVA reactor, Trombay, India). The data were corrected for the background, the empty cell contributions, and the transmission and were placed on an absolute scale using standard protocols. Correction due to

the instrumental smearing was taken into account throughout the data analysis [21]. The differential scattering cross section per unit volume ( $d\Sigma/d\Omega$ ) of monodisperse micelles can be written as [22,23]:

$$\frac{d\Sigma}{d\Omega} = NF_{\text{mic}}(Q)S(Q) + B$$

where,  $N$  is the number density of the micelles and  $B$  is a constant term that represents the incoherent background scattering mainly from the hydrogen present in the sample.  $F_{\text{mic}}(Q)$  is the form factor characteristic of specific size and shape of the scatterers, and  $S(Q)$  is the structure factor that accounts for the interparticle interaction. Core shell micelle a model consisting of PEO chains attached to the surface of the PPO core was considered [22]. The form factor of the micelles  $F_{\text{mic}}(Q)$  comprises four terms: the self-correlation of the core, the self-correlation of the chains, the cross term between the core and chains, and the cross term between different chains. The interparticle structure factor  $S(Q)$  for micelles is captured by the analytical solution of the Ornstein–Zernike equation with the Percus–Yevick approximation [24] employing hard sphere interaction.

#### Nuclear Magnetic Resonance (NMR)

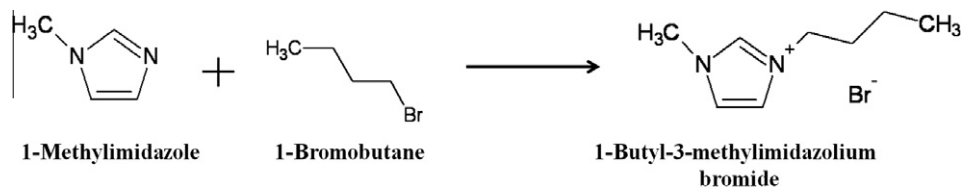
A Bruker AVANCE-II NMR 400.13 MHz spectrometer was used. Solvent suppression eliminated the HDO peak due to residual water. Before being suppressed, the HDO peak was used to calibrate the chemical shift of the spectrum by setting it to 4.65 ppm at 298 K. For NOESY experiments the mixing times and the delay times were estimated from the spin-lattice relaxation times. In all cases, an acquisition delay of  $\gg 3 \times T_1$  and a mixing time of  $\gg 1 \times T_1$  were used to obtain the NOESY spectra. A solution of 5% of copolymer was prepared directly in small sample vials.

#### Preparation of [C<sub>n</sub>mim] [BF<sub>4</sub>]

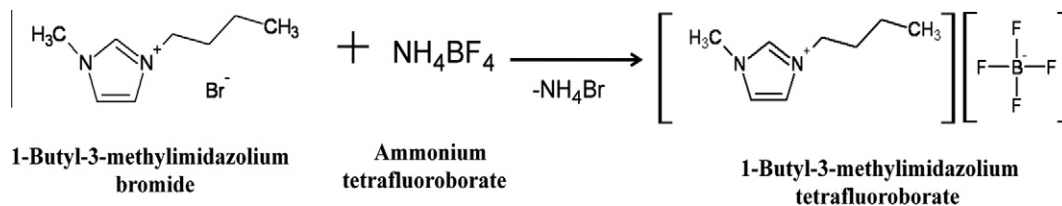
1-Alkyl-3-methylimidazolium bromides were first prepared. The scheme described below for 1-butyl-3-methylimidazolium tetrafluoroborate was followed for other ILs.

1-Butyl-3-methylimidazolium bromide was synthesized. 1-Bromobutane (1.1 mol) was added dropwise into 1-methylimidazole (1 mol) with agitation at 70 °C. The reaction mixture was refluxed for 24 h, and when cooled to room temperature, ethyl acetate was added to the mixture. The ethyl acetate was removed by a separating funnel followed by the addition of fresh ethyl acetate, and this step was repeated four times. The remaining ethyl acetate was removed by rotary evaporation, and the solution was dried under high vacuum at (343–353)K for at least 6 h to get 1-butyl-3-methylimidazolium bromide ([C<sub>4</sub>mim] [Br]) at very high yield (99%) (Scheme 1).

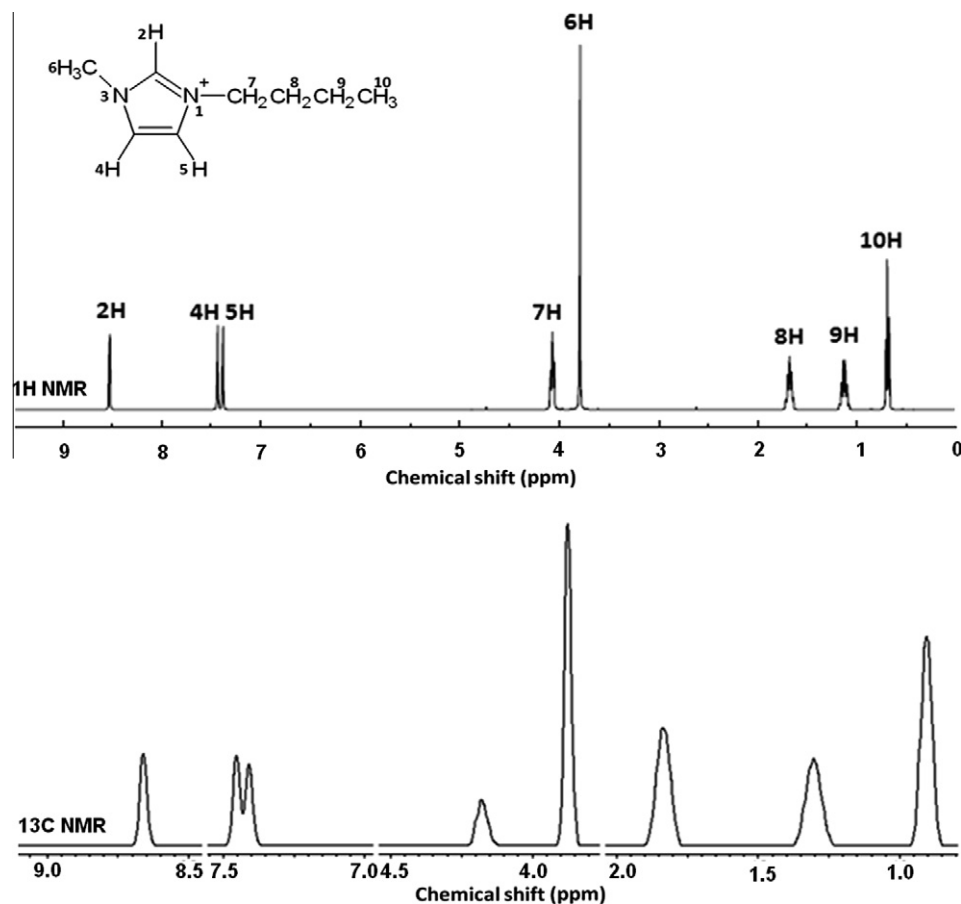
The second step of synthesis of [C<sub>4</sub>mim][BF<sub>4</sub>] is the substitution of the bromide ion with the BF<sub>4</sub><sup>-</sup> ion. Tetrafluoroborate salt was synthesized by metathesis reactions from the corresponding bromide. [C<sub>4</sub>mim][Br] (0.1 mol) was dissolved in acetonitrile (50 mL), and ammonium tetrafluoroborate (0.11 mol) was added. The mixture was refluxed for at least 24 h. When it was cooled to room temperature, NH<sub>4</sub>Br precipitate was removed by filtration. Any remaining precipitate was removed by further filtration at this step. The remaining acetonitrile was removed by rotary evaporation to get crude 1-butyl-3-methylimidazolium tetrafluoroborate. Crude [C<sub>4</sub>mim][BF<sub>4</sub>] was dissolved in dichloromethane (50 mL) and cooled below 278 K. Deionized water and a separation funnel were also cooled to below 278 K. The dichloromethane solution was washed with cooled deionized water (30 mL) five times until the aqueous solution did not form any precipitate with 0.1 mol L<sup>-1</sup> AgNO<sub>3</sub> solution. The solvent dichloromethane was removed by ro-



Scheme 1. Synthesis of 1-Butyl-3-methylimidazolium bromide.



Scheme 2. Synthesis of 1-Butyl-3-methylimidazolium tetrafluoroborate.

Fig. 1.  $^1\text{H}$  NMR and  $^{13}\text{C}$  NMR spectrum of  $\text{C}_4\text{mim BF}_4$  in  $\text{D}_2\text{O}$ .

tary evaporation, and the  $[\text{C}_4\text{mim}][\text{BF}_4]$  was dried under high vacuum at (323–333)K for at least 6 h (Scheme 2).

Fig. 1 shows the  $^1\text{H}$  NMR and  $^{13}\text{C}$  NMR spectrum of  $\text{C}_4\text{mim BF}_4$ . The chemical shifts for  $^1\text{H}$  NMR spectrum (ppm,  $\text{D}_2\text{O}$ ) appear as follows:  $\delta$  8.50 [s, 1H, H(2)], 7.39 [s, 1H, H(4)], 7.350 [s, 1H, H(5)], 4.133 [t, 2H,  $\text{NCH}_2$ ], 3.817 [s, 3H,  $\text{NCH}_3$ ], 1.809 [m, 2H,  $\text{NCH}_2\text{-CH}_2$ ], 1.30 [m, 2H,  $\text{NCH}_2\text{CH}_2\text{-CH}_2$ ], and 0.85 [t, 3H,  $\text{CH}_3$ ].

The  $^{13}\text{C}$  NMR spectrum (ppm,  $\text{D}_2\text{O}$ ) contains peaks:  $\delta$  8.66 [C(2)], 7.46 [C(4)], 7.41 [C(5)], 4.18 [ $\text{N-CH}_2$ ], 3.88 [ $\text{NCH}_3$ ], 1.84 [ $\text{NCH}_2\text{-CH}_2$ ], 1.31 [ $\text{NCH}_2\text{CH}_2\text{-CH}_2$ ], and 0.91 [ $\text{CH}_3$ ]. Impurity peaks

were not observed in the  $^1\text{H}$  NMR and  $^{13}\text{C}$  NMR spectra, and there is a solvent peak at  $\delta$  4.653 in  $^1\text{H}$  NMR spectrum. The chemical shift of other peaks corresponded to structure of the  $[\text{C}_4\text{mim}][\text{BF}_4]$ .

## Results and discussion

### Cloud point

Aqueous solution of PEO-type nonionic surfactants exhibits a cloud point phenomenon [25]; phase separation occurs from

homogeneous solution to two liquid phases, resulting to highly turbid system at a certain temperature. Water molecules interact with nonionic surfactants via van der Waals, hydrogen bonding and hydrophobic hydration. If additives increase hydrophobic hydration in solution more energy is needed to break the hydrogen bonds and the phase separation occurs at higher temperature. This phenomenon is also attributed to the reduction of hydrophilicity of PEO chain caused by the temperature rise. The clouding phenomenon is also observed in  $C_n$ mim type ionic liquids [26].

In Fig. 2 is shown CPs of 5% P103 solutions as a function of the  $C_n$ mim  $BF_4$  concentration.  $C_4$ mim  $BF_4$  and  $C_6$ mim  $BF_4$  (>~1.3%) increase the CP abruptly; such an increase in CP is attributed to different behavior of imidazolium based IL. It exhibits a multiple hydrogen bonding interaction with solute molecules; i.e., butyl methylimidazolium cation acts as a hydrogen-bond donor through H atoms attached to imidazolium ring, while anion species like  $BF_4^-$  acts as a hydrogen bond acceptor [27]. It has been emphasized that the property as a hydrogen-bond acceptor of the counter anion is more important in the solute-solvent interaction in ILs systems [28]. However, in the present case, the oxygen atoms in PEO/PPO chain of the copolymer must play a role as a hydrogen-bond acceptor, and hence, a hydrogen-bond may be formed between imidazolium H atoms in butyl methylimidazolium cation and O atoms in PEO/PPO chain [29,30]. Apart from the PEO oxygen, the terminal OH groups in PEO chain are likely to form hydrogen-bond with  $BF_4^-$  ion. Due to these hydrogen-bond interactions, the solubility of PEO/PPO chain of the copolymer would increase (increase the ionic character), which must be the origin of the increase of CP. In general, the strength of a hydrogen bond interaction reduces with the increase in temperature. Thus, desolvation of the PEO chain would occur at elevated temperature, which brings about the reduced solubility of the nonionic surfactant molecules, and hence, induces a phase separation. This interpretation coincides with the PEO chain length dependence of the cloud point temperature as the case of aqueous system does. The hydrogen bond formation between water and ILs has been reported [31,27].

In the case of  $C_8$ mim  $BF_4$  the increase in the IL concentration, CP once decreases abruptly and then increases. The initial decrease of CP is due to the long chain of  $C_8$ mim  $BF_4$  (water structure maker) which penetrates into P103 micelles and expels the water molecules from the core and enhancing hydrophobic interaction. Considering that  $C_8$ mim  $BF_4$  has a longer alkyl chain than  $C_4$ mim  $BF_4$ , the former can align itself more easily than  $C_4$ mim  $BF_4$  within the P103 micelles by decreasing the hydrophobic hydration while increasing hydrophobic interaction (same behavior was observed

for  $C_6$ mim  $BF_4$  up to ~1.3% concentration). As the concentration of  $C_8$ mim  $BF_4$  increases (>~1.3%), CP again increases due to the reason as discussed above.

#### Dynamic Light Scattering (DLS)

The size and distribution of the aggregates in the mixed system were further examined by DLS. Fig. 3a shows the hydrodynamic diameter ( $D_h$ ), of 5% P103 in aqueous solution and with different concentrations of  $C_n$ mim  $BF_4$  aqueous solutions, at 23 °C.

DLS data (Fig. 3a) show alteration in size, which indicates formation of aggregates involving both P103 and  $C_4$ mim  $BF_4$ . The addition of  $C_4$ mim  $BF_4$  to 5% P103 causes a slight change in the size of micellar aggregates. In the absence of  $C_4$ mim  $BF_4$  the hydrodynamic diameter of the P103 micelles is ~18.5 nm, which is consistent with previous DLS studies [32]. On addition of  $C_4$ mim  $BF_4$ , the size of aggregate slightly increases upto ~28 nm (in presence of ~6.5%  $C_4$ mim  $BF_4$ ). This increase in size is due to the incorporation of  $C_4$ mim  $BF_4$  within P103 micelle which affects the structure of the micelles. Obviously,  $C_4$ mim  $BF_4$  remains as an ion pair within the P103 micelle and goes to the shell (PEO block) region of the micelle. The presence of a large number of the ion pairs in the shell and their electrostatic repulsion may be responsible for the expansion of the shell and, hence, the observed slight increase in the size. Due to the expansion of shell and the penetration of  $C_4$ mim  $BF_4$  (at higher concentration), some monomer of P103 is removed from micelle and can be shown in Fig. 3b in form of size distribution plots. Where monomer peak is observed at higher  $C_4$ mim  $BF_4$  concentration.

The micelle size of P103 remains unchanged in case of  $C_6$ mim  $BF_4$ . The shell region remains unaffected by the addition of  $C_6$ mim  $BF_4$  as it aligns close to core region and hence no observable change in the size. Whereas, the micelle size decreases with the addition of  $C_8$ mim  $BF_4$ .  $C_8$ mim  $BF_4$  is more hydrophobic and relatively less soluble in water. They contributed this to the fact that  $C_8$ mim  $BF_4$  may align itself along with the P103 within the micelles through hydrophobic interactions. This may cause expulsion of water from the mixed micelle causing contraction of size. It seems that the long chain of IL penetrates to PPO core and affects the core. From the above observation it seems that the organic part of the IL plays an important role in the interaction between ILs and P103.

However, the trend in CP and DLS shown by aqueous P103 in the presence of  $C_8$ mim  $BF_4$  is unusual. For  $C_8$ mim  $BF_4$  the CP as well as micelle size decrease upto about 1.3% IL above which an increase in CP is seen though the micelle size still decreases. The initial decrease in CP and size is due to the expulsion of water by the penetration of amphiphilic octyl imidazolium chain. Increase in CP above 1.3% may be accounted for H-bonding between imidazolium cation and PEO unit though the size progressively decrease due to the formation of mixed micelles as observed for Pluronic® in the presence of cationic surfactant [33].

The polydispersity of micelles, evaluated through the ratio  $\mu_2/I^2$  by cumulants analysis, where  $\mu_2$  is the second moment in the cumulants expansion of the correlation function and  $I^2$  is the decay rate, is shown in Table 1. It has been found that the mean diameter of micelles increased from 18.5 nm to 27.8 nm and the polydispersity of micelles increased from 0.045 to 0.27 for  $C_4$ mim  $BF_4$ . For  $C_6$ mim  $BF_4$ , mean diameter of micelles remains almost unchanged (~18.5 nm) but polydispersity is slightly increased. Whereas in case of  $C_8$ mim  $BF_4$  the mean diameter decreases from 18.5 nm to 11.9 nm and polydispersity decreases from 0.22 to 0.13.

#### Small angle neutron scattering (SANS)

The accordingly formed micellar structure was investigated further using SANS. There have been several reports on SANS studies

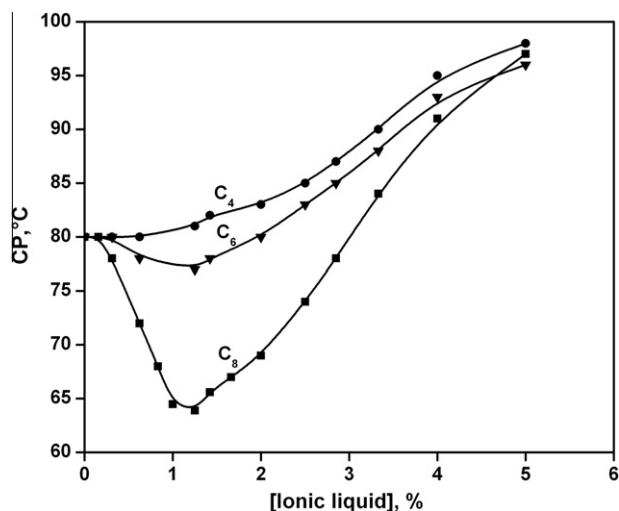


Fig. 2. Cloud point of 5% P103 with varying concentration of  $C_n$ mim  $BF_4$ .

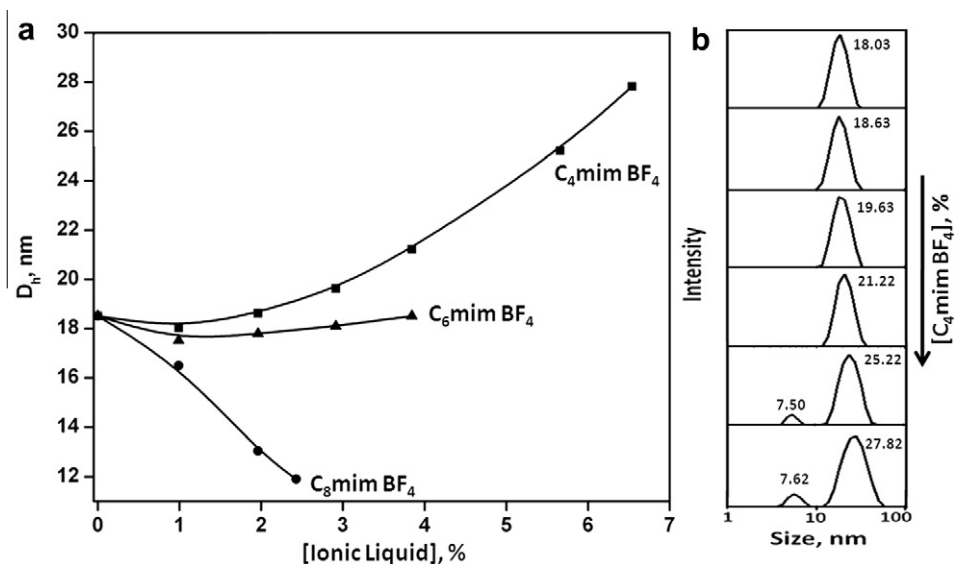


Fig. 3. (a) DLS of 5% P103 as a function of  $C_n$ mim  $BF_4$ , and (b) size distribution plot of 5% P103 as a function of  $C_4$ mim  $BF_4$ .

Table 1

Apparent diameter of P103 micelles (5%) with added  $C_n$ mim  $BF_4$ .

[ $C_4$ mim $BF_4$ ], %	PDI	$D_{hr}$ , nm	[ $C_6$ mim $BF_4$ ], %	PDI	$D_{hr}$ , nm	[ $C_8$ mim $BF_4$ ], %	PDI	$D_{hr}$ , nm
0.00	0.05	18.5	0.00	0.05	18.5	0.0	0.05	18.5
0.99	0.06	18.0	0.99	0.05	17.5	0.99	–	16.5
1.96	0.07	18.6	1.96	0.08	17.8	1.96	0.22	13.0
2.91	0.09	19.6	2.91	0.11	18.1	2.43	0.13	11.9
3.85	0.116	21.2	3.84	0.110	18.5			
5.66	0.176	25.2						
6.54	0.270	27.8						

on PEO–PPO–PEO micelles in water [34,35]. SANS profile for 5% P103 aqueous solution in presence of different concentration of  $C_8$ mim  $BF_4$  at 30 °C is shown in Fig. 4; the lines are model fits using a structural model that is consistent over the concentration regime studied. The mean core radius ( $R_c$ ), radius of gyration of the chain ( $R_g$ ), hard sphere radius, volume fraction of the micelles ( $V_f$ ), aggregation number ( $N_{agg}$ ) and polydispersity of the micelles were determined as the fitting parameters from the analysis. The aggregation number is calculated by the relation  $N = 4\pi ab^2/3v$ , where  $v$  is the volume of the surfactant monomer. Throughout the data

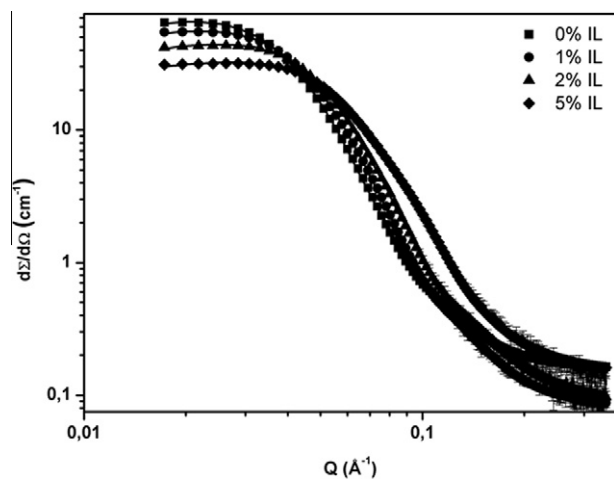


Fig. 4. SANS study of 5% P103 with varying concentration of  $C_8$ mim  $BF_4$  at 30 °C.

analysis corrections were made for instrumental smearing. The radius of gyration of the polymer segment does not show any change in presence of additives, it has been kept fixed (1.4 nm). The analysis of SANS data provides information on shape, size and aggregation number of micelles.

5% P103 at 30 °C contains spherical micelles with aggregation number of 101 and core radius of 5.2 nm. In the presence of 1%  $C_8$ mim  $BF_4$ , the scattering intensity decreases; here the micelles are spherical but aggregation number decreased to 75. However, in presence of 2% and 5%  $C_8$ mim  $BF_4$  aggregation number decreased to 59 and 29, respectively. Thus, the core radius and aggregation number were found to decrease with corresponding increase in  $C_8$ mim  $BF_4$  concentration.

As shown in Fig. 4, the addition of  $C_8$ mim  $BF_4$  shows decrease in scattering profile indicating higher degree of polymer/ $C_8$ mim  $BF_4$  interaction responsible to influence demicellization. The decrease in aggregation number was evidenced, confirming the role of chain length of  $C_8$ mim  $BF_4$ . Due to preferential partitioning in hydrophobic part,  $C_8$ mim  $BF_4$  will interact with the dehydrated PPO blocks. In other words, long chain incorporation to the core takes out

Table 2

Core radius ( $R_c$ ), hard sphere radius ( $R_{hs}$ ) and aggregation number ( $N_{agg}$ ) for 5% P103 with different concentration of ILs.

System	$R_c$ , nm	$R_{hs}$ , nm	$N_{agg}$
5% P103	5.2	8.0	101
5% P103 + 1% $C_8$ mim $BF_4$	4.7	7.4	75
5% P103 + 2% $C_8$ mim $BF_4$	4.2	6.7	59
5% P103 + 5% $C_8$ mim $BF_4$	3.4	5.8	29

Volume fraction ~0.08.

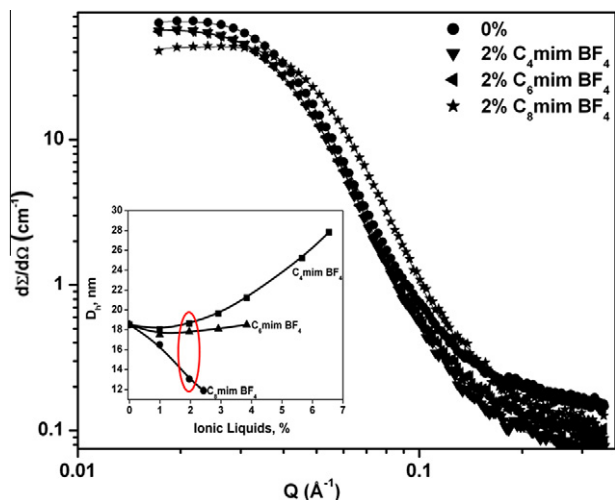


Fig. 5. SANS study of 5% P103 with 2% of  $C_n$ mim  $BF_4$  at 30 °C.

copolymer monomer, which is responsible for the decrease in size. Fig. 4 shows higher scattered intensity due to the formation of micelle in the solution. Lower scattered intensity is attributed to the unimer in solution [36]. The increase in the scattered intensity can be understood in terms of change in the contrast  $(\rho_m - \rho_s)^2$  between the micelle and the solvent. However, an increase in neutron-scattering intensity is due to an increase in the size of the PPO core and not an increase in the number density of micelles.

Upon addition of 1%, 2% and 5%  $C_8$ mim  $BF_4$  the micelle size decreases as the addition of  $C_8$ mim  $BF_4$  destroys the aggregates of P103. Due to the hydrogen bond and hydrophobic interactions between P103 and  $C_8$ mim  $BF_4$ ,  $C_8$ mim<sup>+</sup> cations align within the P103 micelles to form mixed micelles. On one hand, it enhances the electrostatic repulsion between PEO groups of P103 and the other hand due to the preferential partitioning in hydrophobic part,  $C_8$ mim  $BF_4$  will interact with dehydrated PPO blocks. Therefore electrostatic repulsion opens up the micelle and long chain of  $C_8$ mim  $BF_4$  molecules permeate into PPO block and remove P103 monomer and thus decrease in the size of P103. These results are in agreement to DLS study. SANS data for solutions of  $C_8$ mim  $BF_4$  with varying concentrations are given in Table 2. The corresponding volume fractions are also given.

Further, we have compared the effect of each ILs (2%) on 5% P103. From Fig. 5 it can be seen that intensity of (5% P103 +  $C_8$ mim  $BF_4$ ) is slightly less than pure P103 and also less than P103 in presence of  $C_4$ mim  $BF_4$  and  $C_6$ mim  $BF_4$ . Furthermore the hard sphere radius, core radius and aggregation number clearly shows the difference in size of P103 in presence of  $C_8$ mim  $BF_4$  and  $C_4$ mim  $BF_4$ ,  $C_6$ mim  $BF_4$ . The clear indication can be obtained from aggregation number (Table 3) where the  $N_{agg}$  of 5% P103 and 5% P103 in presence of  $C_4$ mim  $BF_4$ ,  $C_6$ mim  $BF_4$  is almost same compared to P103 in presence of  $C_8$ mim  $BF_4$ . These results indicate that there is not much change in micelle size in presence of  $C_4$ mim  $BF_4$  and  $C_6$ mim  $BF_4$

**Table 3**  
Comparison of core radius ( $R_c$ ), hard sphere radius ( $R_{hs}$ ) and aggregation number ( $N_{agg}$ ) for 5% P103 in presence 2%  $C_n$ mim  $BF_4$ .

System	$R_c$ , nm	$R_{hs}$ , nm	$N_{agg}$
5% P103	5.2	8.0	101
5% P103 + 2% $C_4$ mim $BF_4$	5.2	7.9	98
5% P103 + 2% $C_6$ mim $BF_4$	5.1	7.8	95
5% P103 + 2% $C_8$ mim $BF_4$	4.2	6.7	59

Volume fraction  $\sim 0.07$ .

whereas  $C_8$ mim  $BF_4$  decreases micelle size which are in good agreement to results obtained from DLS (as can be seen in red circle in inset of Fig. 5).

## NOESY

The microstructure and structural change of the P103 micelles can be outlined by this method to a certain extent, although it is difficult to determine the precise interproton distances between each individual proton from the cross-peak intensities of the NOESY spectrum. The location of ILs in P103 micelles was determined by using NOESY which is an excellent noninvasive technique [37,38]. A representative NOESY spectrum is shown in Fig. 6. Significant positive cross peaks observed indicate the closeness of the protons between the IL and P103.

Strong correlation between PPO ( $\delta = 1.0$  ppm) methyl protons and 8-H ( $\delta = 1.3$ ), 9-H ( $\delta = 1.6$ ), protons of the imidazolium cation can be seen. It suggests that there is interaction between the PPO block and butyl group of imidazolium cation. Moreover, interactions between 2-H, 4-H, 5-H ( $\delta = 7.4$ – $7.5$ ) protons and PEO ( $\delta = 3.7$  ppm) methyl protons are also observed. This indicates interaction of PEO and imidazolium cation. It is seen that 6-H, 7-H, 10-H protons and protons of P103 overlap each other, which shows that they have similar environment. No discussion can however be made on interaction between these protons due to overlap between signals.

Those results indicate that when  $C_4$ mim  $BF_4$  is added to the P103 aqueous solution, the organic cations of the  $C_4$ mim  $BF_4$  are embedded in the micelle core through the hydrophobic interaction between PPO blocks and butyl group of the  $C_4$ mim<sup>+</sup>. With the increase of  $C_4$ mim concentration, more and more  $C_4$ mim<sup>+</sup> are embedded in the micelles, so that the Pluronic® P103 micelles become bigger. As has been reported [39] that RTILs are not likely to dissociate in its aqueous solution (except at infinite dilution), it can be deduced that the  $C_4$ mim<sup>+</sup> is embedded into P103 micelle with  $BF_4$  connected to it, so the addition of the ionic liquids has little effect on the bulk water, and thus the properties of P103 is almost unchanged.

Based on the results of CP, DLS, SANS and 2D NMR, the structure of the mixed micelles formed by  $C_n$ mim  $BF_4$ /P103 and their interaction and location is illustrated in Scheme 3.

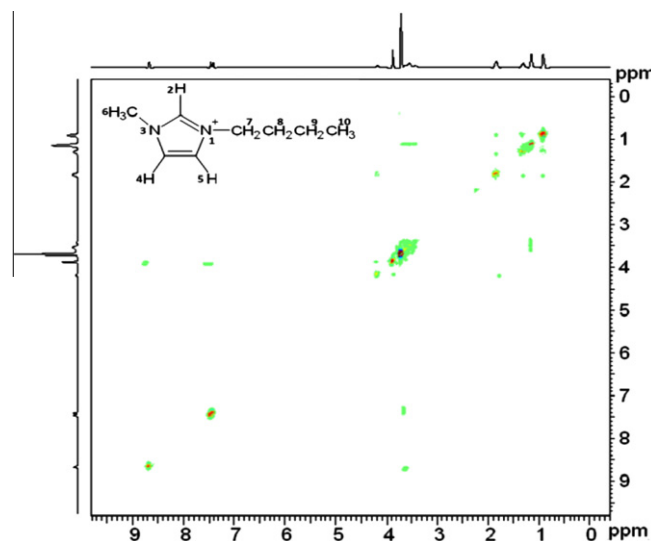
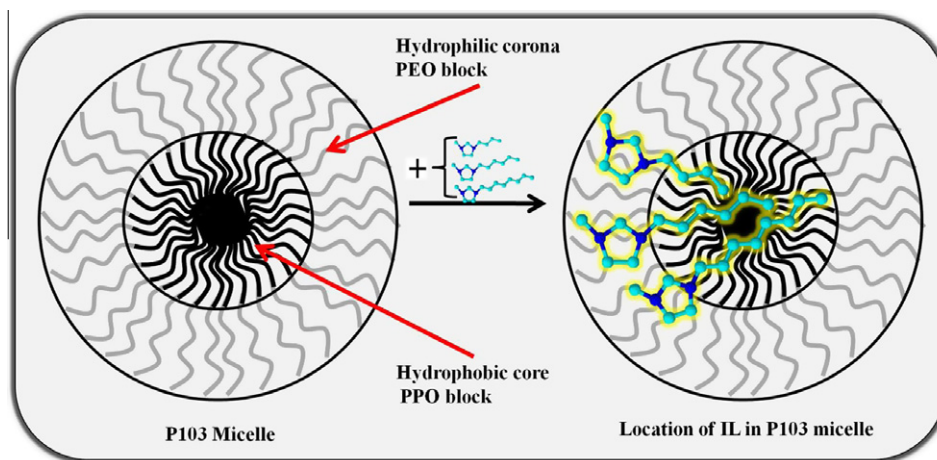


Fig. 6. NOESY for 5% P103 +  $C_4$ mim  $BF_4$  system.



Scheme 3. Possible location of ILs in P103 micelle.

## Conclusions

The CP, DLS, SANS and NMR studies show that addition of the ILs  $C_n\text{mim BF}_4$  to aqueous P103 micellar solution affects the solution behavior. The measurements revealed that ILs can increase CP of P103 dramatically. This could be due to (i) hydrogen-bond interactions between the imidazolium cation of the ionic liquid and PEO units of P103 and (ii) hydrophobic interactions between the alkyl chain of the imidazolium cation and the hydrophobic chain of P103. The DLS results showed the size alteration; with  $C_4\text{mim BF}_4$ , the micelle size increases as the electrostatic repulsion between PEO groups of P103 is increased due to the permeation of imidazolium cation and forms bigger aggregates. With  $C_6\text{mim BF}_4$  the micelle size of P103 remains unchanged where the shell region remains unaffected by the addition of  $C_6\text{mim BF}_4$  as it aligns close to core region and hence no observable change in the size. For  $C_8\text{mim BF}_4$ , the micelle size of P103 increases due to the fact that  $C_8\text{mim BF}_4$  may align itself along with the P103 micelle and may cause expulsion of water from the mixed micelle causing contraction of size. SANS data are in good agreement to the results observed from the DLS. The selective NOESY spectrum indicates that the PPO block of P103 interacts with the butyl group of the imidazolium cation by hydrophobic interaction.

The data strongly indicate partitioning of  $C_n\text{mim BF}_4$  into micellar phase and formation of mixed micelles. The presence of IL within the micelles results in enhanced dipolarity with significantly altering CP, micelle size and aggregation number. This may turn out to be fairly useful in many applications involving micellar media.

## References

- [1] P. Wasserscheid, T. Welton, *Ionic Liquids in Synthesis*, vol. 1, Springer, 2008.
- [2] M.J. Earle, K.R. Seddon, *Pure Appl. Chem.* 72 (2000) 1391–1398.
- [3] O.A. El Seoud, P.A.R. Pires, T. Abdel-Moghny, E.L. Bastos, *J Colloid Interface Sci.* 313 (2007) 296.
- [4] J. Bowers, C.P. Butts, P.J. Martin, M.C. Vergara-Gutierrez, *Langmuir* 20 (2004) 2191–2198.
- [5] T. Singh, M. Drechsler, A.H.E. Müller, I. Mukhopadhyay, A. Kumar, *Phys. Chem. Chem. Phys.* 12 (2010) 11728–11735.
- [6] P.D. Galgano, O.A. El Seoud, *J Colloid Interface Sci.* 345 (2010) 1–11.
- [7] J. Łuczak, C. Jungnickel, I. Łačka, S. Stoltec, J. Hupkaa, *Green Chem.* 12 (2010) 593–601.
- [8] J. Wang, H. Wang, S. Zhang, H. Zhang, Y. Zhao, *J. Phys. Chem. B* 111 (2007) 6181–6188.
- [9] A. Kumar, T. Singh, R.L. Gardas, J.A.P. Coutinho, *J. Chem. Therm.* 40 (2008) 32–39.
- [10] N. Li, S. Zhang, L. Zheng, B. Dong, X. Li, Li Yu, *Phys. Chem. Chem. Phys.* 10 (2008) 4375–4377.
- [11] K. Nakashima, P. Bahadur, *Adv. Colloid Interface Sci.* 123–126 (2006) 75–96.
- [12] D.A. Chiappetta, A. Sosnik, *Eur. J. Pharm. Biopharm.* 66 (2007) 303–317.
- [13] A. Tercjak, E. Serrano, I. Garcia, I. Mondragon, *Acta Mater.* 56 (2008) 5112–5122.
- [14] T. Inoue, T. Misono, *J. Colloid Interface Sci.* 337 (2009) 247–253.
- [15] T. Inoue, H. Yamakawa, *J. Colloid Interface Sci.* 356 (2011) 798–802.
- [16] D.K. Das, A.K. Das, T. Mondal, A.K. Mandal, K. Bhattacharyya, *J. Phys. Chem. B* 114 (2010) 13159–13166.
- [17] A. Adhikari, S. Dey, D. Kumar Das, U. Mandal, S. Ghosh, K. Bhattacharyya, *J. Phys. Chem. B* 112 (2008) 6350–6357.
- [18] Y. Gao, N. Li, X. Li, S. Zhang, L. Zheng, X. Bai, L. Yu, *J. Phys. Chem. B* 113 (2009) 123–130.
- [19] L. Zheng, C. Guo, J. Wang, X. Liang, S. Chen, J. Ma, B. Yang, Y. Jiang, H. Liu, *J. Phys. Chem. B* 111 (2007) 1327–1333.
- [20] Z. Bai, T.P. Lodge, *Langmuir* 26 (2010) 8887–8892.
- [21] V.K. Aswal, P.S. Goyal, *Curr. Sci.* 79 (2000) 947–953.
- [22] J.S. Pedersen, C. Gerstenberg, *Macromolecules* 29 (1996) 1363–1365.
- [23] J.S. Pedersen, *J. Appl. Crystallogr.* 33 (2000) 637–640.
- [24] J.K. Percus, G. Yevick, *J. Phys. Rev.* 110 (1958) 1.
- [25] M.J. Rosen, *Surfactants and Interfacial Phenomena*, second ed., Wiley, New York, 1989.
- [26] C. Patrascu, F. Gauffre, Fr. Nallet, R. Bordes, J. Oberdisse, N. de Lauth-Viguerie, C. Mingotaud, *Chem. Phys. Chem.* 7 (2006) 99–101.
- [27] K.A. Fletcher, S. Pandey, *J. Phys. Chem. B* 107 (2003) 13532–13539.
- [28] J.L. Anderson, J. Ding, T. Welton, D.W. Armstrong, *J. Am. Chem. Soc.* 124 (2002) 14247–14254.
- [29] S. Zhang, Y. Gao, B. Dong, L. Zheng, *Colloids Surf. A: Physicochem. Eng. Aspects* 372 (2010) 182–189.
- [30] T.G.A. Youngs, J.D. Holbrey, M. Deetlefs, M. Nieuwenhuyzen, M.F.C. Gomes, C. Hardacre, *Chem. Phys. Chem.* 7 (2006) 2279–2281.
- [31] J.N.C. Lopes, M.F.C. Gomes, A.A.H. Pádua, *J. Phys. Chem. B* 110 (2006) 16816–16818.
- [32] P. Parekh, K. Singh, D.G. Marangoni, P. Bahadur, *J. Mol. Liquids* 165 (2012) 49–54.
- [33] J. Mata, T. Joshi, D. Varade, G. Ghosh, P. Bahadur, *Colloid Surf. A: Physicochem. Eng. Aspects* 247 (2004) 1.
- [34] Y. Liu, S. Chen, S. Chen, J.S. Huang, *Macromolecules* 31 (1998) 2236–2244.
- [35] I. Goldmints, F.K. Gottberg, K.A. Smith, T.A. Hatton, *Langmuir* 13 (1997) 3659–3664.
- [36] V.K. Aswal, P.S. Goyal, J. Kohalbrecher, P. Bahadur, *Chem. Phys. Lett.* 349 (2001) 458–462.
- [37] G. Wang, G. Olofsson, *J. Phys. Chem. B* 102 (1998) 9276–9283.
- [38] S.Z. Mao, Y.R. Du, *Acta Phys. Chim. Sin.* 19 (2003) 675–680.
- [39] K. Miki, P. Westh, K. Nishikawa, Y. Koga, *J. Phys. Chem. B* 109 (2005) 9014–9019.